microRNA-7 Inhibits the Epidermal Growth Factor Receptor and the Akt Pathway and Is Down-regulated in Glioblastoma

Benjamin Kefas,[1] Jakub Godlewski,[2] Laurey Comeau,[1] Yunqing Li,[1] Roger Abounader,[1] Michael Hawkinson,[1] Jeongwu Lee,[3] Howard Fine,[3] E. Antonio Chiocca,[2] Sean Lawler,[2] and Benjamin Purow[1]

[1]Division of Neuro-Oncology, Neurology Department, University of Virginia Health System, Charlottesville, Virginia; [2]Dardinger Laboratory for Neuro-Oncology and Neurosciences, Department of Neurological Surgery, Ohio State University Medical Center, Columbus, Ohio; and [3]Neuro-Oncology Branch, National Cancer Institute, NIH, Bethesda, Maryland

Abstract

microRNAs are noncoding RNAs inhibiting expression of numerous target genes, and a few have been shown to act as oncogenes or tumor suppressors. We show that microRNA-7 (miR-7) is a potential tumor suppressor in glioblastoma targeting critical cancer pathways. miR-7 potently suppressed epidermal growth factor receptor expression, and furthermore it independently inhibited the Akt pathway via targeting upstream regulators. miR-7 expression was down-regulated in glioblastoma versus surrounding brain, with a mechanism involving impaired processing. Importantly, transfection with miR-7 decreased viability and invasiveness of primary glioblastoma lines. This study establishes miR-7 as a regulator of major cancer pathways and suggests that it has therapeutic potential for glioblastoma. [Cancer Res 2008;68(10):3566–72]

Introduction

microRNAs (miRNAs or miRs) are recently discovered short RNAs regulating gene expression in normal tissues and cancer. Located in introns or intergenic regions, a large primary microRNA (pri-microRNA) is transcribed and then processed to a pre-microRNA hairpin. pre-microRNA is processed in the cytoplasm to yield mature microRNA, which targets genes with complementary sites in the 3′- or 5′-untranslated region (UTR; refs. 1, 2). Complementarity to the microRNA "seed" region at its 5′-end seems necessary. microRNAs usually inhibit translation of targets but sometimes trigger cleavage of target mRNA (3). Up-regulated and down-regulated microRNAs have been observed in several tumors, including brain tumors such as glioma and its aggressive glioblastoma subtype (4). Some targets of these microRNAs have been identified, such as RAS for let-7 and bcl-2 for miR-15/16, but microRNA regulators of critical cancer proteins and pathways largely remain unknown (5, 6).

Our work with Notch in gliomas led us to investigate microRNA-7 (miR-7), previously shown to suppress Notch target genes in *Drosophila* (7). We noticed binding sites for the human miR-7 homologue in the epidermal growth factor receptor (EGFR) 3′-UTR. Little has been published on miR-7, which is replicated at three locations in the human genome. Interestingly, it was reported in the *Drosophila* retina that EGFR indirectly regulates miR-7 (8). Herein, we show for the first time that miR-7 potently and directly regulates EGFR. Furthermore, we show that the Akt pathway critical in glioblastomas and other cancers is also directly inhibited by miR-7. Not surprisingly given these effects, we found marked down-regulation of miR-7 in glioblastoma. Further experiments implicated decreased processing of the three pri-miR-7 isoforms as a mechanism. Additionally, miR-7 transfection impaired viability and invasiveness of glioma lines. Taken together, these results establish miR-7 as a regulator of EGFR expression and Akt pathway activity down-regulated in glioblastoma, with potential therapeutic implications.

Materials and Methods

Cell culture. Established glioma lines U87MG, T98G, and A172 were acquired from the American Type Culture Collection, whereas primary lines GBM10 and GBM6 were a gift from Jann Sarkaria (Mayo Clinic, Rochester, MN; ref. 9). Tumor stem cell line 0308 was derived and validated as described previously (10). All lines were grown under previously described conditions.

Materials. pre-microRNAs were purchased from Ambion. EGFR and insulin receptor substrate (IRS)-2 short interfering RNAs (siRNA) were from Santa Cruz Biotechnology and control siRNA was from Qiagen. The wild-type (wt) EGFR and EGFR vIII vectors were a kind gift of Sarah Parsons (University of Virginia, Charlottesville, VA; ref. 11).

Plasmid construction. 3′-UTR reporter plasmids were constructed via insertion of the EGFR 3′-UTR, the IRS-2 3′-UTR, or three copies of the full site complementary to miR-7 into the *Xba*I restriction site 3′ to luciferase in the pGL3-promoter plasmid (Promega Corp.). For EGFR and IRS-2 3′-UTRs, these regions were amplified from human genomic DNA and cloned into the pCRII-TOPO plasmid (Invitrogen) before splicing into pGL3-promoter.

The pri-miR-7-2 vector contains pre-miR-7-2 with 600 bp flanking sequences in the pCRII-TOPO plasmid; the sequence was amplified from genomic DNA with the following primers: 5′-GGAAGAGAGAAATGAGCCACTTGC-3′ and 5′-GTATTCCTGCCACAGTGGGGGATG-3′.

Cell transfection. siRNA transfections used Oligofectamine reagent as described previously (Invitrogen; ref. 12). microRNA transfections were performed similarly but with 20 nmol/L microRNA instead of 10 nmol/L siRNA. For 0308 tumor stem cells, the plates were first coated with laminin/poly-L-ornithine (Sigma-Aldrich Co.). Transfection of plasmids was done with Fugene HD (Invitrogen) per the manufacturer's instructions. For U87, we used Fugene (Invitrogen). Plasmid transfections were in six-well plates with 0.5 μg of reporter plasmid plus 0.05 μg cytomegalovirus-β-galactosidase or with 1.5 μg of pri-miR-7-2/control plasmid.

Real-time PCR to quantify mature, pri-miR-7, and pre-miR-7. Patient samples were obtained with an Ohio State University Institutional Review Board–approved protocol. Total RNA was extracted with Trizol (Invitrogen). For endogenous controls, cDNA was synthesized using random hexamers with iScript cDNA Synthesis kit (BioRad) and 1 μg total RNA. For mature microRNA expression analysis, cDNA was synthesized using Taqman MicroRNA Reverse Transcription kit (Applied Biosystems) and 10 ng total RNA along with miR-7–specific primer supplied with miR-7 Taqman MicroRNA Assay (Applied Biosystems). Quantitative real-time PCR analysis was performed using the 7500 Real-Time PCR System (Applied Biosystems).

Requests for reprints: Benjamin Purow, University of Virginia Neuro-Oncology Center, Box 800434, Hospital West Complex 6th Floor, Charlottesville, VA 22908. Phone: 434-924-5545; Fax: 434-243-6843; E-mail: bwp5g@virginia.edu.

doi:10.1158/0008-5472.CAN-07-6639

A human 18S rRNA Taqman probe (Applied Biosystems) was used as endogenous control.

For miR-7-1, miR-7-2, and miR-7-3 precursors and primary transcripts, expression analysis was performed as described (13) using 7500 Real-Time PCR System, Power SYBR Green Master Mix (both Applied Biosystems), and human 18S rRNA primers (forward, 5′-AACTTTCGATGGTAGTCGCCG-3′; reverse, 5′-CCTTGGATGTGGTAGCCGTTT-3′) as endogenous control. A similar strategy was used to quantitate primary transcripts with the pan-mir-7 primer from Jiang et al. and the following primers: pri-miR-7-1, 5′-GTAAGGTGTGAAATGCTGCA-3′; pri-miR-7-2, 5′-AAAAAGAACACGTGGAAGGATAG-3′; and pri-miR-7-3, 5′-TGTATCGCCTGGAGTGAGC-3′.

Immunoblots. Western blots were performed as described (12). Primary antibodies included anti-EGFR, IRS-1, glyceraldehyde-3-phosphate dehydrogenase-horseradish peroxidase (GAPDH-HRP; Santa Cruz Biotechnology), IRS-2, total Akt, and phospho-Akt (Ser^{473}; Cell Signaling Technology). HRP-conjugated secondary antibodies were from Jackson Immunology Labs (1:10,000).

Alamar Blue assay. One-tenth volume of Alamar Blue (BioSource) was added and plates were incubated at 37°C until pinkness was noted. Fluorescence was measured with excitation at 550 nm and emission at 590 nm on a Wallac Victor 1420 Multilabel Counter (Perkin-Elmer).

Cell cycle analysis. Propidium iodide/bromodeoxyuridine (BrdUrd) cell cycle assay was performed as described (12) with flow cytometry on a FACSVantage SE (Becton Dickinson).

Luciferase assay. Luciferase reporter assays were performed as described on a Promega GloMax 20/20 luminometer (12). Luciferase activity was double normalized by dividing each well first by β-galactosidase activity and then by average luciferase/β-galactosidase value in a parallel set done with constitutive luciferase plasmid.

Cell invasion assay. Invasion assays were performed as described (14).

Statistics. Student's t test was performed with Microsoft Office Excel 2003.

Results and Discussion

miR-7 directly inhibits EGFR expression via its 3′-UTR. We assessed complementarity of miR-7 to the EGFR 3′- and 5′-UTRs, finding several seed matches of bases 1 to 8 and 1 to 7 in the 3′-UTR (Fig. 1*A*). To assess miR-7 inhibition of EGFR, glioma cells were transfected with pre-miR-7 or control pre-miR. We tested the efficiency of our pre-miR-7 transfection with a miR-7 activity reporter, a plasmid containing three fully complementary miR-7 target sites as a 3′-UTR for the *luciferase* gene. Transfection with pre-miR-7 ablated reporter activity ($P < 0.001$; Fig. 1*B*), indicating high transfection efficiency and efficacy. Immunoblot showed profoundly decreased EGFR protein (Fig. 1*C*). Consistent with translational inhibition by microRNAs, we noted decreased EGFR protein and not mRNA (real-time PCR data not shown). Corroborating the effects of miR-7 on EGFR with another modality, we showed that transfection with a pri-miR-7-2 vector decreased EGFR protein in HeLa cells (Fig. 1*C*). To confirm direct action of miR-7 on the EGFR 3′-UTR, we synthesized a reporter plasmid with the 3′-UTR behind luciferase. Transfection with miR-7 inhibited normalized activity of the EGFR 3′-UTR reporter by ~83% ($P < 0.01$; Fig. 1*D*), a striking decrease relative to similar experiments in the literature (15, 16).

miR-7 suppresses Akt pathway activation independent of its EGFR inhibition. EGFR and Akt play central roles in glioblastoma. We noted that, in addition to targeting EGFR, miR-7 also includes among its predicted targets upstream regulators of the Akt pathway, such as IRS-1 and IRS-2. The effect of miR-7 transfection on Akt activity was determined by immunoblot for Akt phosphorylated at Ser^{473}, frequently used as a surrogate marker for Akt activity. pre-miR-7 transfection decreased Akt phosphorylation and thus Akt activation (Fig. 2*A*). Investigating further, we performed immunoblot for IRS-1 and IRS-2, which contain target sites for miR-7 in their 3′-UTRs (Fig. 2*B*). pre-miR-7 transfection of glioma cells decreased expression of both IRS-1 and IRS-2 protein (Fig. 2*C*). To show direct regulation of IRS-2 by miR-7, we synthesized a luciferase/IRS-2 3′-UTR reporter and showed that miR-7 transfection reduced its activity ($P < 0.05$; Fig. 2*C*). As evidence that IRS-2 regulates Akt activity in glioma cells, we validated commercially available siRNA to IRS-2 and showed that knockdown of IRS-2 with this siRNA in a glioma line decreased phospho-Akt on immunoblotting (Fig. 2*C*).

EGFR has been reported to up-regulate Akt activity in certain settings (17). Although we showed that upstream regulators of Akt were targets of miR-7, we sought to further show that the effects of miR-7 on Akt activity were not indirect via EGFR inhibition. To address this, we determined the effects on Akt phosphorylation of transfecting the same glioma lines with an EGFR siRNA. The reduction in EGFR protein by this siRNA resembled that with miR-7 (Fig. 2*D*), but it did not decrease Akt phosphorylation. Because EGFR knockdown by another modality did not affect Akt activation, it supports the contention that miR-7 inhibits Akt activation independent of its effects on EGFR. We also showed that "EGFR rescue" with vectors delivering wt EGFR or the constitutively active EGFR vIII mutant, both lacking the EGFR 3′-UTR and thus insensitive to miR-7, could not ablate the decrease in phospho-Akt caused by miR-7 (Fig. 2*D*).

miR-7 expression is decreased in glioblastomas through reduced processing. Given the inhibition of miR-7 of EGFR and the Akt pathway, we hypothesized that its expression would be suppressed in glioblastoma. Using modified real-time PCR to quantitate mature miR-7 in five human glioblastomas and adjacent normal brain, we found its expression markedly decreased in glioblastomas ($P < 0.01$; Fig. 3*A*). This is consistent with a report assessing microRNA expression in the NCI-60 cell lines relative to corresponding normal tissues; miR-7 was among the microRNAs decreased in glioblastoma lines (18).

We then considered mechanisms for the decreased miR-7 expression. Among the miR-7 isoforms, miR-7-1 and miR-7-3 are located within introns of the *HNRPK* and *PGSF1* genes, respectively, whereas miR-7-2 is intergenic. We used online microarray data (from databases REMBRANDT and ONCOMINE) to compare approximate mRNA expression of the miR-7-1 and miR-7-3 host genes in patient samples of glioblastoma versus normal brain (data not shown). *PGSF1*, the host gene for miR-7-3, showed lower expression in glioblastoma. However, both databases showed comparable or higher expression of *HNRPK*, the miR-7-1 host gene, in glioblastoma versus normal brain. This suggested that decreased transcription of the host gene was not responsible for the decreased expression, at least for miR-7-1. We then sequenced all three pre-miR-7 regions in several glioma cell lines to identify mutations or deletions. No deletions were noted. Although we found a few isolated point mutations within 300 to 400 bases of the pre-miR-7s, none was within the pre-miR-7s themselves (data not shown). These results implied that other mechanisms were responsible.

To dissect expression and processing of miR-7, we used modified real-time PCR to quantitate pri- and pre- forms of all three miR-7 isoforms in the glioblastoma/brain samples (two complete sets shown in Fig. 3*B*). Notably, levels of pri-miR-7s were generally similar in glioblastoma and normal brain, whereas levels of pre-miR-7s were decreased (Fig. 3*B*). This suggested that glioblastomas

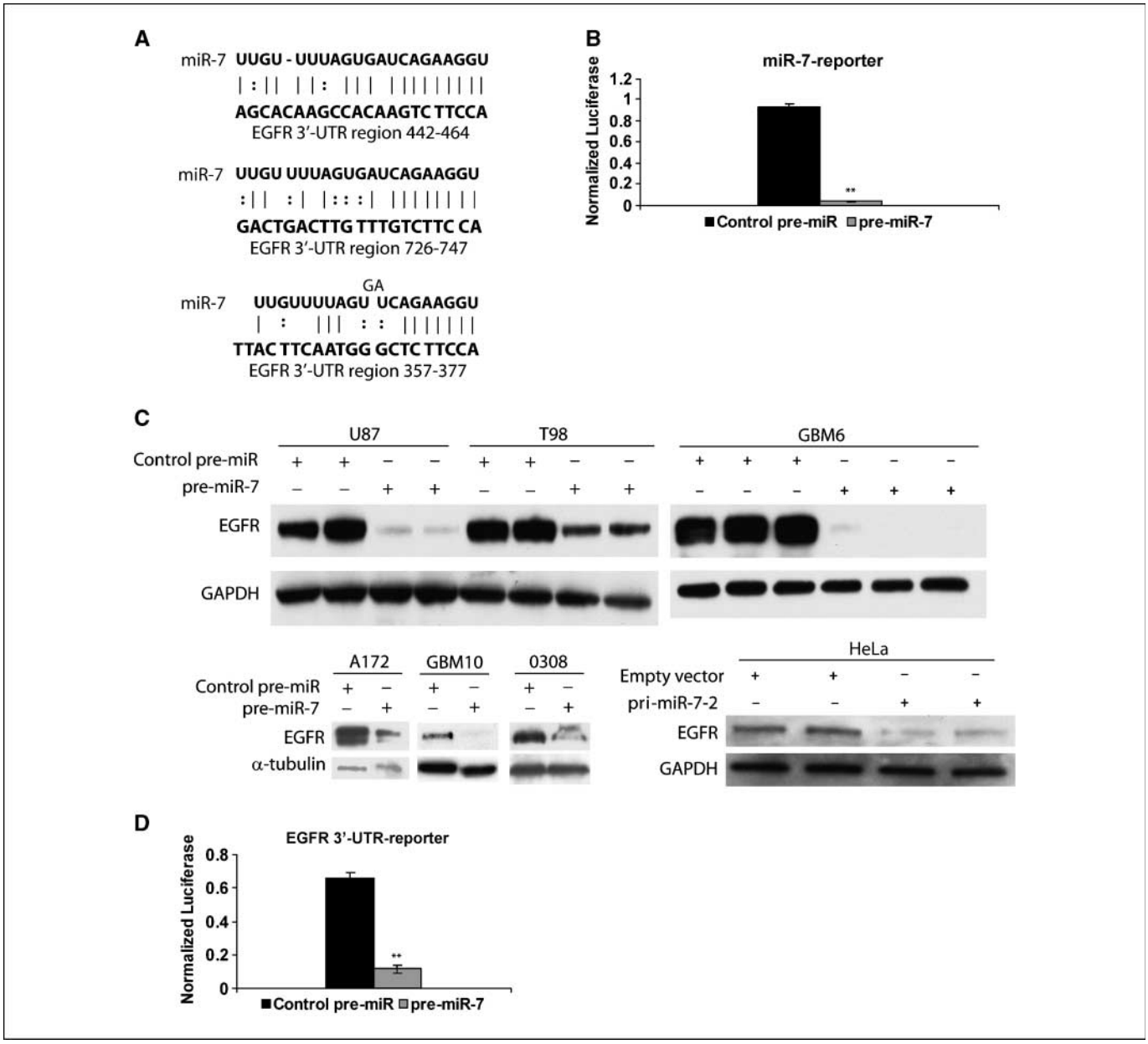

Figure 1. miR-7 directly inhibits EGFR expression. *A,* sites of miR-7 seed matches in the EGFR 3′-UTR. *B,* normalized activity of a miR-7 activity reporter in the U87MG glioma line 3 d after transfection of pre-miR-7 or control miR. **, $P < 0.01$. *C,* immunoblot of EGFR protein in established (U87MG, T98G, and A172), primary (GBM6 and GBM10), and tumor stem cell (0308) glioma lines 3 d after transfection with pre-miR-7 or control pre-miR. *Bottom,* GAPDH or α-tubulin loading controls. Immunoblot of EGFR protein in the HeLa cervical carcinoma line 3 d after transfection with pri-miR-7-2 vector or empty vector control. *Bottom,* GAPDH loading controls. *D,* normalized activity of an EGFR 3′-UTR luciferase reporter in the U87MG glioma line 3 d after transfection of pre-miR-7 or control miR.

have a processing defect in generating pre-miR-7 from pri-miR-7 in all three isoforms.

To further investigate the prospect of a processing defect, we synthesized a pri-miR-7-2 vector. This allowed comparison of pri-miR-7 or pre-miR-7 transfection in a glioblastoma line versus a different cancer line. If the defect in miR-7 expression in glioblastoma lay in processing from pri-miR-7 to pre-miR-7, we expected transfection with the pri- form but not the pre- form to be less effective in the glioblastoma line versus the other line. This indeed proved true. Using our EGFR 3′-UTR luciferase reporter to gauge miR-7 activity, we found that pre-miR-7 was similarly effective in U87MG and HeLa cells, but pri-miR-7-2 was markedly less efficient in the glioma line versus the cervical cancer line (Fig. 3*C*). This was not due to lesser transfectability of the glioblastoma line to plasmids, as the raw luciferase and β-galactosidase values were much higher than in the cervical cancer line (luciferase values shown in Fig. 3*C*). Consistent with these results, transfection with the pri-miR-7 vector did not result in decreased EGFR or phospho-Akt protein in U87MG cells (Fig. 3*C*), in contrast to the effects of this vector on EGFR protein in HeLa cells (Fig. 1*C*). It should also be noted that although we do not show that the defect in glioblastoma microRNA processing is selective and not global, this is indicated by reports showing pronounced overexpression of some microRNAs in glioblastoma versus normal brain (4, 19).

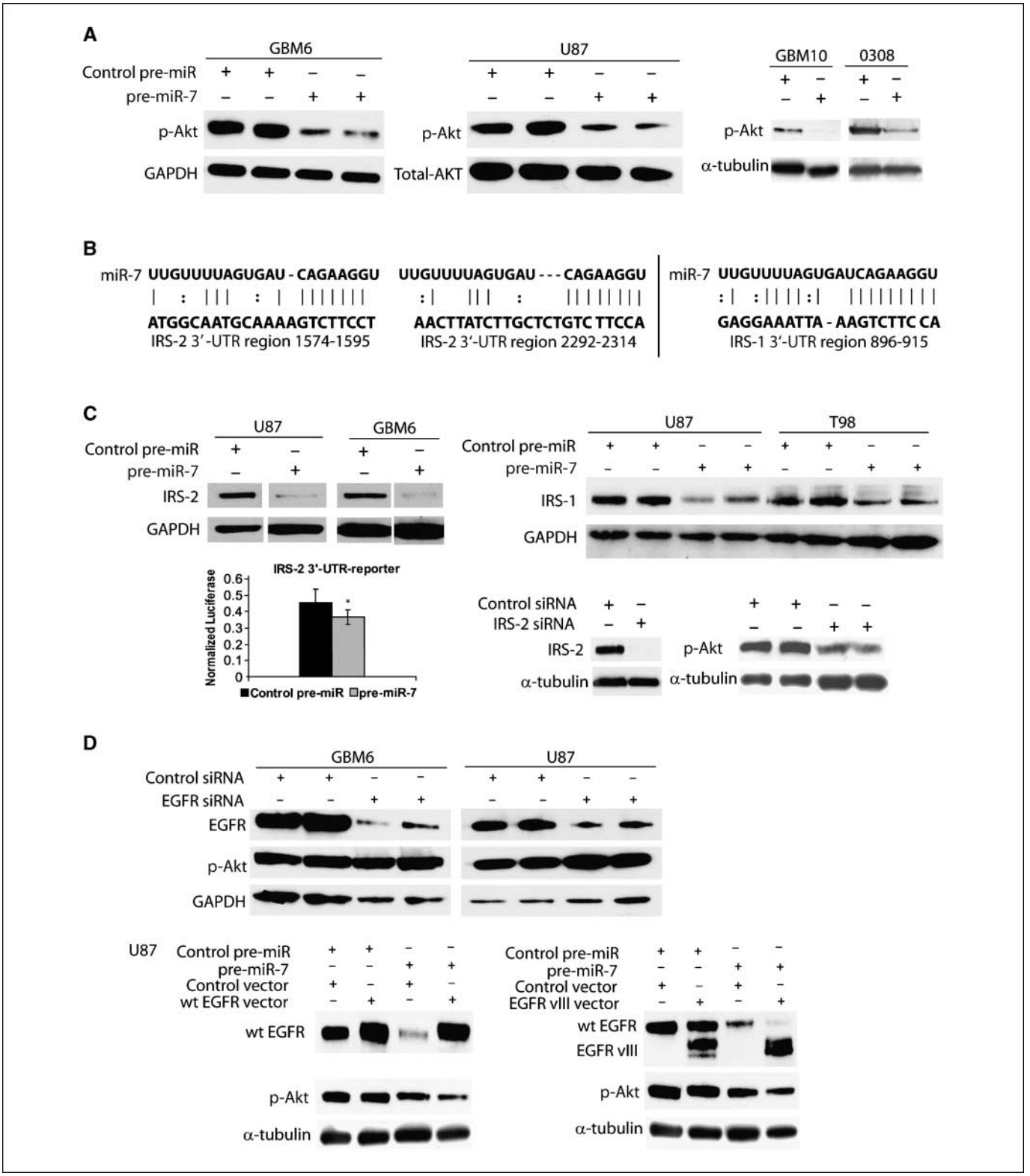

Figure 2. miR-7 inhibits the Akt pathway through targeting of pathway members. *A,* immunoblot of phospho-Akt (Ser^{473}) in established (U87MG), primary (GBM6 and GBM10), and tumor stem cell (0308) glioma lines 3 d after transfection with pre-miR-7 or control pre-miR. *Bottom,* total Akt, GAPDH, or α-tubulin loading controls. *B,* sites of miR-7 seed matches in the IRS-2 and IRS-1 3′-UTRs. *C,* immunoblots of IRS-2 and IRS-1 proteins in established (U87MG and T98G) and primary (GBM6) glioma lines 3 d after transfection with pre-miR-7 or control pre-miR. *Bottom,* GAPDH loading controls. Normalized activity of an IRS-2 3′-UTR luciferase reporter in the U87MG glioma line 3 d after transfection of pre-miR-7 or control miR. **, $P < 0.01$. Also shown are immunoblots for IRS-2 and phospho-Akt (Ser^{473}) in U87MG cells 3 d after transfection with control or IRS-2 siRNA. *Bottom,* α-tubulin loading controls. *D,* immunoblots of EGFR and phospho-Akt proteins in established (U87MG) and primary (GBM6) glioma lines 3 d after transfection with EGFR siRNA or control siRNA. *Bottom,* GAPDH loading controls. Also shown are immunoblots for EGFR and phospho-Akt in U87MG cells transfected 3 d earlier with pre-miR-7 or control pre-miR and with either control vector, wt EGFR vector, or constitutively active mutant EGFR vIII vector. *Bottom,* α-tubulin loading controls.

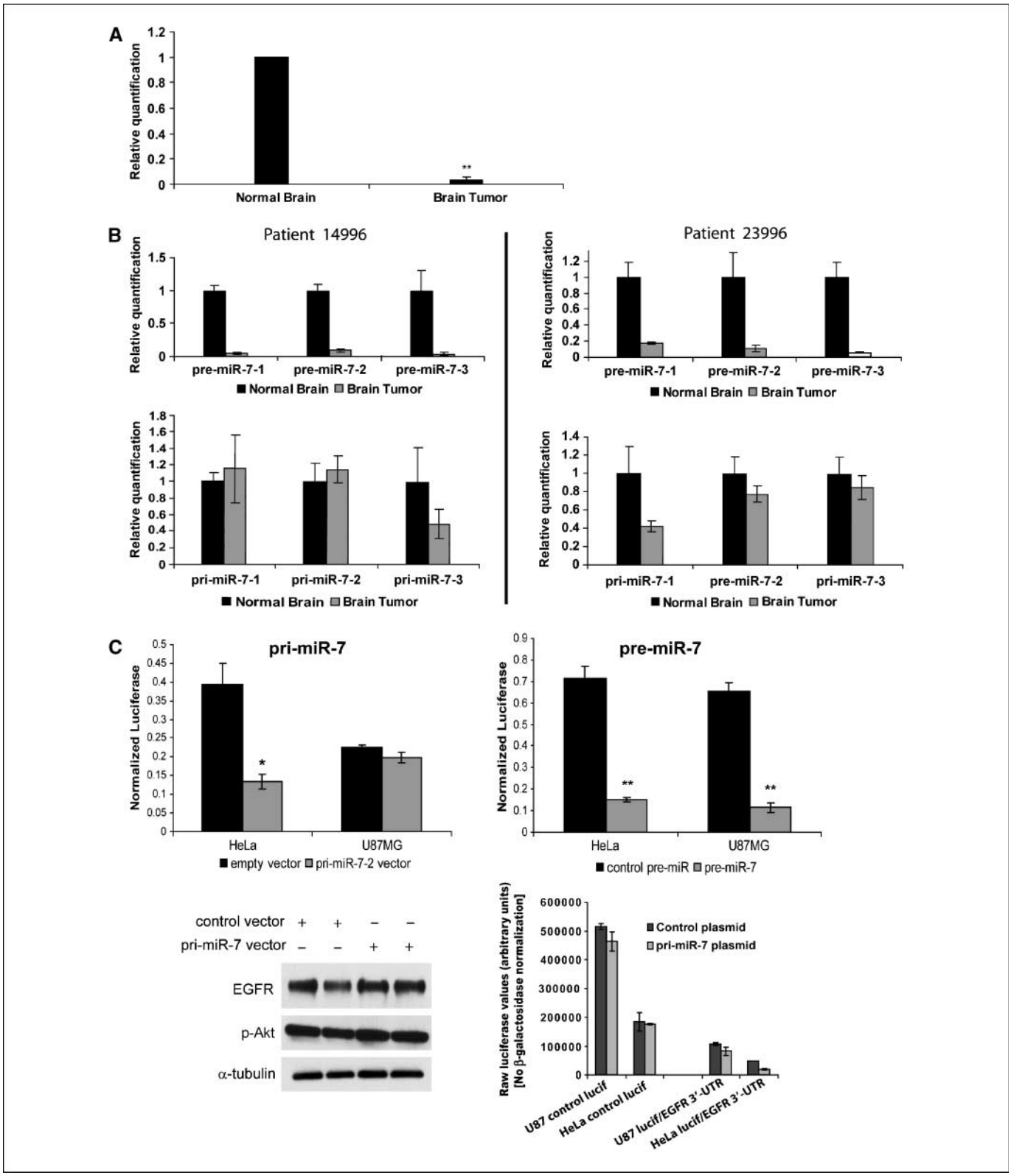

Figure 3. miR-7 expression is down-regulated in glioblastomas relative to normal brain through a processing deficiency. *A,* plot of mean expression of mature miR-7 by real-time PCR in five glioblastoma samples relative to normal brain samples from the same patients. Mean from brain samples normalized to 1. **, $P < 0.01$. *B,* expression of pre-miR-7-1, pre-miR-7-2, and pre-miR-7-3 and of pri-miR-7-1, pri-miR-7-2, and pri-miR-7-3 by real-time PCR in glioblastoma and normal brain from two patient samples. Values from control brain samples normalized to 1. *C,* normalized activity of the EGFR 3′-UTR luciferase reporter in the U87MG glioma line and the HeLa cervical carcinoma cell line 3 d after transfection of pri-miR-7-2 vector or empty vector control. Shown adjacent for comparison is an analogous experiment but with transfection of pre-miR-7 or control pre-miR instead of pri-miR-7-2 vector or control vector. Raw luciferase values following pri-miR-7 transfection (and without β-galactosidase normalization) are displayed. Also shown are immunoblots of EGFR and phospho-Akt (Ser^{473}) in U87MG cells 3 d after transfection with control or pri-miR-7-2 vector.

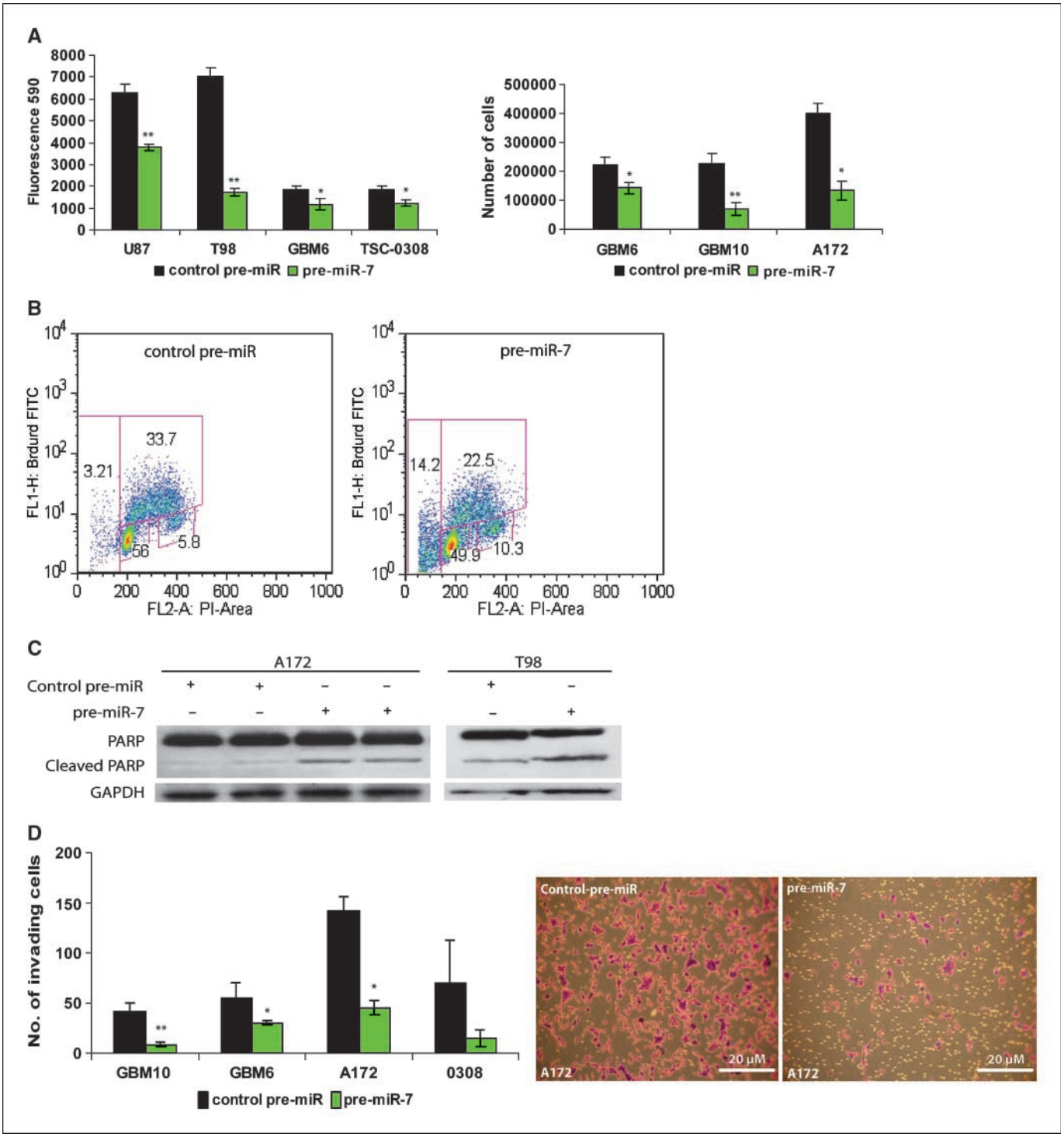

Figure 4. Transfection with miR-7 inhibits glioma cell proliferation, survival, and invasiveness. *A,* results of Alamar Blue assay of cell viability performed 5 to 7 d after transfection with pre-miR-7 or control pre-miR in established (U87MG and T98G), primary (GBM6), or tumor stem cell (0308) glioma lines. Cell counts performed 5 to 7 d after transfection with pre-miR-7 or control pre-miR in established (A172) and primary (GBM6 and GBM10) glioma lines. *, $P < 0.05$; **, $P < 0.01$. *B,* propidium iodide (*PI*)/BrdUrd FITC cell cycle assay results of T98G glioma cells 3 d after transfection with pre-miR-7 or control pre-miR. *C,* immunoblots of PARP protein in established (A172 and T98G) glioma lines 3 d after transfection with pre-miR-7 or control pre-miR. *Bottom,* GAPDH loading controls. *D,* plots showing mean number of invading cells in established (A172), primary (GBM6 and GBM10), and tumor stem cell (0308) glioma lines 3 d after transfection with pre-miR-7 or control pre-miR. Photomicrographs of a sample Transwell membrane with invading A172 cells are shown.

miR-7 decreases viability and invasiveness of glioblastoma cells. The effects of miR-7 on critical glioblastoma pathways and its down-regulation suggested that delivering this miR might have therapeutic utility in glioblastoma. We therefore evaluated the effects of transient transfection of pre-miR-7 or control in glioma cells. Alamar Blue assay, a redox assay similar to 3-(4,5-dimethylthiazol-2-yl)-2,5-diphenyltetrazolium bromide (MTT), showed significant decreases following pre-miR-7 transfection in established

glioma lines (U87MG and T98G), a primary glioma line (GBM6), and an established glioblastoma "stem-like" line (0308; Fig. 4*A*). In addition, cell counts were significantly decreased in glioma lines following transfection with pre-miR-7 (Fig. 4*A*). Cell cycle assay following pre-miR-7 transfection indicated a marked increase in the sub-G_0 apoptotic fraction (from 2.2% to 14%), a decrease in the S fraction (from 34.6% to 22.3%), and an increase in G_2-M arrest (from 4.89% to 10.1%; Fig. 4*B*). Further supporting apoptosis, pre-miR-7 transfection increased cleaved poly(ADP-ribose) polymerase (PARP; Fig. 4*C*).

EGFR and Akt activity have been associated with glioblastoma invasiveness, a central characteristic behind its lethality. The inhibition of both pathways by miR-7 indicated that it might also diminish glioblastoma invasiveness. Transfection with pre-miR-7 indeed decreased invasion through collagen IV–coated Transwells for both established and primary glioma cell lines, with a similar trend in a glioblastoma stem cell line (Fig. 4*D*).

Given the centrality of EGFR and the Akt pathway in glioblastomas, delivery of miR-7 may represent an appealing approach for therapy. The fact that transient transfection of miR-7 had therapeutic effects not only in established glioma lines but also in primary lines and a tumor stem cell line is encouraging. miR-7 delivery is likely to be safe in normal brain, given its regular expression there. Efforts are currently under way to develop the therapeutic potential of miR-7 in animal models of glioblastoma.

Disclosure of Potential Conflicts of Interest

No potential conflicts of interest were disclosed.

Acknowledgments

Received 12/14/2007; revised 2/7/2008; accepted 2/29/2008.

The costs of publication of this article were defrayed in part by the payment of page charges. This article must therefore be hereby marked *advertisement* in accordance with 18 U.S.C. Section 1734 solely to indicate this fact.

We thank Joanne Lannigan and Michael Solga for assistance with flow cytometry, Jann Sarkaria for his kind gift of primary glioblastoma lines, and Tom Schmittgen for guidance on real-time PCR of microRNAs.

References

1. Lytle JR, Yario TA, Steitz JA. Target mRNAs are repressed as efficiently by microRNA-binding sites in the 5′ UTR as in the 3′ UTR. Proc Natl Acad Sci U S A 2007;104:9667–72.
2. Lai EC. Micro RNAs are complementary to 3′ UTR sequence motifs that mediate negative post-transcriptional regulation. Nat Genet 2002;30:363–4.
3. Yekta S, Shih IH, Bartel DP. MicroRNA-directed cleavage of HOXB8 mRNA. Science 2004;304:594–6.
4. Ciafre SA, Galardi S, Mangiola A, et al. Extensive modulation of a set of microRNAs in primary glioblastoma. Biochem Biophys Res Commun 2005;334:1351–8.
5. Johnson SM, Grosshans H, Shingara J, et al. RAS is regulated by the let-7 microRNA family. Cell 2005;120:635–47.
6. Cimmino A, Calin GA, Fabbri M, et al. miR-15 and miR-16 induce apoptosis by targeting BCL2. Proc Natl Acad Sci U S A 2005;102:13944–9.
7. Lai EC, Tam B, Rubin GM. Pervasive regulation of *Drosophila* Notch target genes by GY-box-, Brd-box-, and K-box-class microRNAs. Genes Dev 2005;19:1067–80.
8. Li X, Carthew RW. A microRNA mediates EGF receptor signaling and promotes photoreceptor differentiation in the *Drosophila* eye. Cell 2005;123:1267–77.
9. Giannini C, Sarkaria JN, Saito A, et al. Patient tumor EGFR and PDGFRA gene amplifications retained in an invasive intracranial xenograft model of glioblastoma multiforme. Neuro Oncol 2005;7:164–76.
10. Lee J, Kotliarova S, Kotliarov Y, et al. Tumor stem cells derived from glioblastomas cultured in bFGF and EGF more closely mirror the phenotype and genotype of primary tumors than do serum-cultured cell lines. Cancer Cell 2006;9:391–403.
11. Tice DA, Biscardi JS, Nickles AL, Parsons SJ. Mechanism of biological synergy between cellular Src and epidermal growth factor receptor. Proc Natl Acad Sci U S A 1999;96:1415–20.
12. Purow BW, Haque RM, Noel MW, et al. Expression of Notch-1 and its ligands, Delta-like-1 and Jagged-1, is critical for glioma cell survival and proliferation. Cancer Res 2005;65:2353–63.
13. Jiang J, Lee EJ, Gusev Y, Schmittgen TD. Real-time expression profiling of microRNA precursors in human cancer cell lines. Nucleic Acids Res 2005;33:5394–403.
14. Amos S, Mut M, diPierro CG, et al. Protein kinase C-α-mediated regulation of low-density lipoprotein receptor related protein and urokinase increases astrocytoma invasion. Cancer Res 2007;67:10241–51.
15. He L, He X, Lim LP, et al. A microRNA component of the p53 tumour suppressor network. Nature 2007;447:1130–4.
16. le Sage C, Nagel R, Egan DA, et al. Regulation of the p27(Kip1) tumor suppressor by miR-221 and miR-222 promotes cancer cell proliferation. EMBO J 2007;26:3699–708.
17. Li B, Yuan M, Kim IA, Chang CM, Bernhard EJ, Shu HK. Mutant epidermal growth factor receptor displays increased signaling through the phosphatidylinositol-3 kinase/AKT pathway and promotes radioresistance in cells of astrocytic origin. Oncogene 2004;23:4594–602.
18. Gaur A, Jewell DA, Liang Y, et al. Characterization of microRNA expression levels and their biological correlates in human cancer cell lines. Cancer Res 2007;67:2456–68.
19. Chan JA, Krichevsky AM, Kosik KS. MicroRNA-21 is an antiapoptotic factor in human glioblastoma cells. Cancer Res 2005;65:6029–33.

microRNA-7 Inhibits the Epidermal Growth Factor Receptor and the Akt Pathway and Is Down-regulated in Glioblastoma

Benjamin Kefas, Jakub Godlewski, Laurey Comeau, et al.

Cancer Res 2008;68:3566-3572.